RESEARCH ARTICLE

# Ecological traits of planktonic viruses and prokaryotes along a full-salinity gradient

Yvan Bettarel[1], Thierry Bouvier[1], Corinne Bouvier[1], Claire Carré[1], Anne Desnues[2], Isabelle Domaizon[3], Stéphan Jacquet[3], Agnès Robin[4] & Télesphore Sime-Ngando[4]

[1]IRD, UMR 5119 ECOSYM, Montpellier, France; [2]IRD, UMR 6535 LOPB, Marseille, France; [3]INRA, UMR 42 CARRTEL, Thonon-les-Bains, France; and [4]CNRS, UMR 6023, Aubière, France

**Correspondence:** Yvan Bettarel, Université de Montpellier 2 – CC 093, Montpellier, 34095 cedex 5, France. Tel.: +33 4 67 14 39 98; fax: + 33 4 67 14 37 19; e-mail: yvan.bettarel@ird.fr

Received 18 June 2010; revised 13 December 2010; accepted 17 January 2011.
Final version published online 14 February 2011.

DOI:10.1111/j.1574-6941.2011.01054.x

Editor: Patricia Sobecky

**Keywords**
virus; salinity; prokaryote; aquatic; lysogeny; SHOW.

## Abstract

Virus–prokaryote interactions were investigated in four natural sites in Senegal (West Africa) covering a salinity gradient ranging from brackish (10‰) to near salt saturation (360‰). Both the viral and the prokaryote communities exhibited remarkable differences in their physiological, ecological and morphological traits along the gradient. Above 240‰ salinity, viral and prokaryotic abundance increased considerably with the emergence of (1) highly active square haloarchaea and of (2) viral particles with pleiomorphic morphologies (predominantly spindle, spherical and linear shaped). Viral life strategies also showed some salinity-driven dependence, switching from a prevalence of lytic to lysogenic modes of infection at the highest salinities. Interestingly, the fraction of lysogenized cells was positively correlated with the proportion of square cells. Overall, the extraordinary abundance of viruses in hypersaline systems (up to $6.8 \times 10^8$ virus-like particles per milliliter) appears to be partly explained by their high stability and specific ability to persist and proliferate in these apparently restrictive habitats.

## Introduction

Planktonic viruses are of tremendous ecological relevance because of their lytic capacities within each of the three domains of life (Eubacteria, Archaea and Eukarya), their extraordinary abundance and diversity, and their effects on biogeochemical cycles in the hydrosphere (Suttle, 2005). Among the physical factors that influence their distribution directly or indirectly, salinity is assumed to be among the most crucial (Oren, 2009), alongside UV radiation (Wilhelm *et al.*, 2003) and temperature (Bettarel *et al.*, 2009). Salinity was initially recognized for its remarkable relationship with the diversity and functions of prokaryotes, which are the usual hosts of aquatic viruses (Bouvier & del Giorgio, 2002; Cissoko *et al.*, 2008; Boetius & Joye, 2009). Bacteria and Archaea were indeed thought to be physiologically, genetically and ecologically dependent on external osmolarity (Lozupone & Knight, 2007). For example, marine prokaryotes have long been known to be remarkably halotolerant, which allows them to live in habitats with a wide range of osmolarities and ion compositions (Forsyth *et al.*, 1971). Typically, prokaryotes respond to osmotic stress by adjusting their cell turgor (Oren, 2002; Shabala *et al.*, 2009), either by increasing the synthesis of a variety of organic 'compatible' osmolytes or by controlling the fluxes of ions across cell membranes (Sleator & Hill, 2001). However, at salinity levels in excess of 250‰, the osmotic stress becomes so high that only a very limited number of prokaryotic species can thrive, including the hyperhalophilic bacterium *Salinibacter ruber* (Antón *et al.*, 2002; Rosselló-Mora *et al.*, 2008) and the square haloarchaea of Walsby (SHOW), well known for its singular postage stamp morphology (Walsby, 2005; Cuadros-Orellana *et al.*, 2007). Such extremophile prokaryotes have attracted considerable interest in recent decades, and they have been identified in various types of hypersaline waters such as solar salterns (Antón *et al.*, 2002) and soda lakes (Sorokin & Kuenen, 2005), located in different regions of the world including Australia (Burns *et al.*, 2007), Israel (Oren, 2002), Spain (Guixa-Boixareu *et al.*, 1996) and Peru (Maturrano *et al.*, 2006). Numerous reports regarding their cultivation, genetic features and metabolic properties have provided new insights into life at the biological limits of salt tolerance (Bolhuis *et al.*, 2006; Burns *et al.*, 2007).

Although the impact of salinity on prokaryote ecology has been fairly well documented, only a handful of studies have explored whether this parameter is also a strong determinant of viral abundance and diversity distribution in water. From recent reports, we know that viral abundance can increase drastically as the salt concentration increases, reaching up to $10^9$ viruses per milliliter in systems where NaCl is close to saturation, such as crystallizer ponds (Guixa-Boixareu *et al.*, 1996) and hypersaline lakes (Oren *et al.*, 1997; Brum *et al.*, 2005; Bettarel *et al.*, 2010). Conversely, the diversity of viruses together with that of their main prokaryotic hosts have been shown to decrease along increasing salinity gradients (Sandaa *et al.*, 2003; Auguet *et al.*, 2006). Currently, the reasons for the high densities of viruses in hypersaline waters are still poorly understood. The salt-forced extinction of potential virivorous nanoflagellates (Pedrós-Alió *et al.*, 2000; Bettarel *et al.*, 2005) is a possible explanation, but the ability of these viruses to better resist ambient UV radiations is not unrealistic either. Extreme halophilic Archaea and Bacteria could also be more susceptible to viral infection than their low-salinity counterparts. Furthermore, we still totally lack information on how viral life strategies may be influenced by salinity. The lytic, lysogenic and chronic cycles of infection are the main paths through which phages manipulate microbial processes, biogeochemical cycles and gene transfer (Weinbauer, 2004; Rohwer & Thurber, 2009). Because virus–prokaryote interactions are strongly dependent on the physiological state of the host (Maurice *et al.*, 2010), we can anticipate that salinity is likely to exert a strong influence on the replication strategies used by prokaryotic viruses. However, it is still unclear whether hypersaline environments and their highly specific prokaryotic flora are more favorable to one or the other phage life cycles. These questions have never been addressed and they are fundamental to unveil the role played by salinity in structuring aquatic microbial food webs. Finally, previous studies on phage distribution along salinity gradients have been reported exclusively at temperate latitudes and mostly along restricted portions of the gradient. More systematic studies are thus required to elucidate host–virus interactions along full-salinity gradients, primarily in tropical ecosystems. Indeed, during the past two decades, biophysicochemical data provided by multidisciplinary studies have consistently revealed that aquatic ecology in temperate zones is somewhat different from that in tropical systems (Talling & Lemoalle, 1998). For instance, because of the typically high bacterial growth rates mostly resulting from the high temperatures encountered in tropical regions, trophic pathways within microbial food webs are not readily homologous in the two zones (Bouvy *et al.*, 2004). The same conclusion is expected to be reached regarding virus-mediated processes.

In this study, we take advantage of four discontinuous aquatic sites located in Senegal, covering a full-salinity gradient from the same thalassohaline origin (i.e. the Senegalese coastal waters of the Atlantic Ocean), to examine virus–prokaryote interactions during the late dry season. By screening multiple physiological, ecological, morphological and phylogenetic traits of viral and prokaryotic communities, our main objective was to evaluate how these two communities can survive, interact and proliferate in water where the salt concentration increases up to saturation.

## Materials and methods

### Study sites

Samples were collected in Senegal (West Africa) from four aquatic sites contrasted in their salinity levels. These sites were sampled within an area encompassed between the Gambian border to the South and by the Senegal River to the north (Fig. 1). All the four sites share water from the same origin: the coastal Atlantic Ocean, and are therefore thalassohaline. A total of 14 sampling stations were identified within the four sites covering the full range of salinity from brackish (10‰) to near salt saturation (360‰).

The stations with salinity 10‰, 20‰ and 30‰ (named S.10, S.20 and S.30) were selected along the estuary of Senegal River (Fig. 1), which is among the longest rivers on the North West coast of Africa, running over 1800 km through four countries: Guinea, Mali, Mauritania and Senegal, where it flows into the Atlantic Ocean through a delta, which forms a complex canal system. Stations S.40, S.60, S.80, S.100 and S.120 were sampled in the Saloum River estuary, which has become an inverse estuary since the late 1960s with salinity that increases upstream and reaches 120‰ in some places. This unusual phenomenon is the result of the intrusion of coastal waters due to shallow estuarine slopes and a combination of insignificant freshwater flows (as a result of the Sahelian drought) and very high evaporation levels (more details in Diop *et al.*, 1997). Stations S.140, S.190 and S.240 were investigated in artisanal saltern ponds located on the Saloum River bank, 3 km from the city of Kaolack. Finally, stations S.290, S.330 and S.360 were sampled in the hypersaline Lake Retba. This lake (surface area: ~400 ha) is located near Dakar (30 km), has shallow lagoon-like features with a maximum depth of 3 m and is located in close proximity (400 m) to the Atlantic Ocean. The high salinity of the Lake Retba (also known as the *Pink Lake*) results from severe evaporation that exceeded the input of water (from the sea) in a basin formerly connected to the sea (Garnier, 1978). The lake also receives some infiltration of freshwater, resulting locally in a steep salinity gradient ranging from *c.* 300‰ to salt saturation

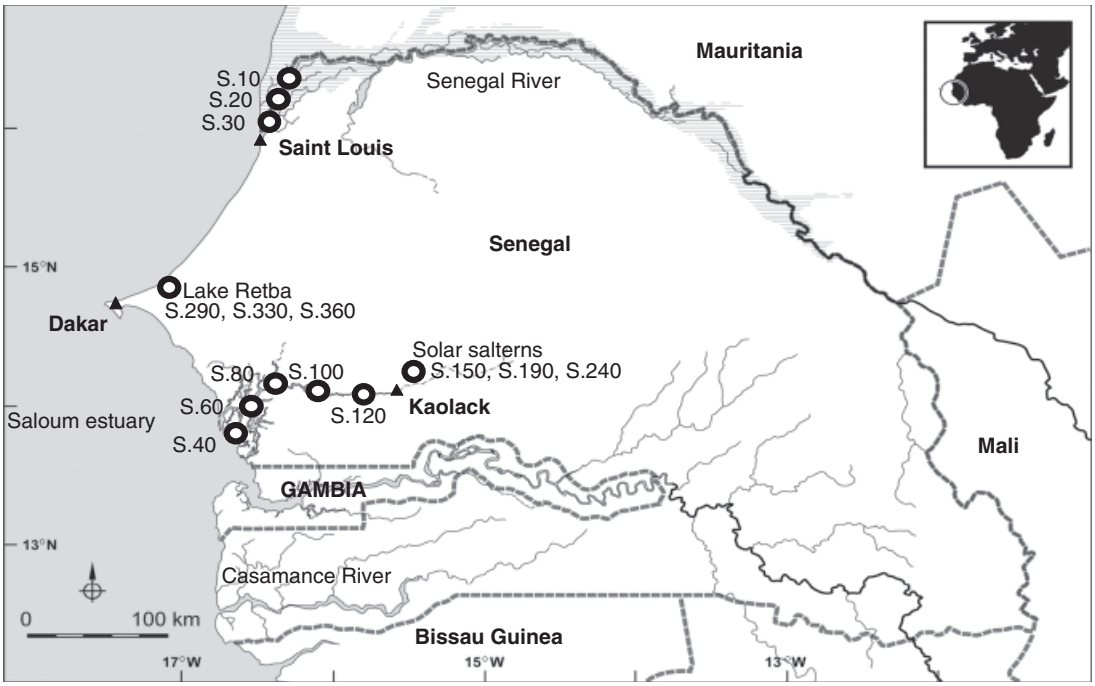


**Fig. 1.** Map of Senegal and the location of the sampling stations.

**Table 1.** Geographical coordinates and physicochemical parameters at the 14 sampled stations in Senegal (West Africa), May 2007

| Station | Site | Salinity (‰) | Latitude north | Longitude west | Temperature (°C) | $PO_4^-$ (μM) | $NO_3^-+NO_2^-$ (μM) | $NH_4^+$ (μM) | Chlorophyll (μg $L^{-1}$) |
|---|---|---|---|---|---|---|---|---|---|
| S.10 | Senegal estuary | 10 | 16°13′01″ | 16°25′08″ | 23.2 | 0.2 | 5.2 | 2.4 | 4.7 |
| S.20 | Senegal estuary | 20 | 16°11′54″ | 16°26′47″ | 23.3 | 0.2 | 1.5 | 0.6 | 6.0 |
| S.30 | Senegal estuary | 30 | 16°05′03″ | 16°27′12″ | 23.3 | 0.4 | 10.1 | 1.6 | 12.1 |
| S.40 | Saloum estuary | 40 | 14°00′24″ | 16°41′52″ | 22.9 | 0.1 | 2.8 | 0.8 | ND |
| S.60 | Saloum estuary | 60 | 14°08′10″ | 16°26′57″ | 23.4 | 0.1 | 0.9 | 0.5 | 2.5 |
| S.80 | Saloum estuary | 80 | 14°11′47″ | 16°26′24″ | 24.7 | 0.0 | 1.2 | 0.3 | 3.0 |
| S.100 | Saloum estuary | 100 | 14°12′42″ | 16°25′12″ | 24.8 | 0.0 | 0.9 | 0.9 | 2.1 |
| S.120 | Saloum estuary | 120 | 16°16′08″ | 16°22′15″ | 25.2 | 0.0 | 0.9 | 0.8 | 2.2 |
| S.140 | Solar salterns (Kaolack) | 140 | 14°06′55″ | 15°59′38″ | 29.3 | 0.0 | 3.7 | 5.6 | 0.4 |
| S.190 | Solar salterns (Kaolack) | 190 | 14°06′54″ | 15°59′35″ | 29.1 | 0.0 | 0.9 | 79.6 | 19.0 |
| S.240 | Solar salterns (Kaolack) | 240 | 14°06′53″ | 15°59′36″ | 29.1 | 0.0 | 1.8 | 1.1 | 1.7 |
| S.290 | Retba Lake | 290 | 14°54′14″ | 17°14′55″ | 27.2 | 1.7 | 1.9 | 0.3 | 33.5 |
| S.330 | Retba Lake | 330 | 14°50′14″ | 17°14′55″ | 27.1 | 0.8 | 4.4 | 0.0 | 6.1 |
| S.360 | Retba Lake | 360 | 14°50′14″ | 17°14′54″ | 26.7 | 6.3 | 1.3 | 0.0 | 4.8 |

ND, not determined.

(370‰) at the end of the dry season. The geographical coordinates of the different stations are presented in Table 1.

## Sampling

Samples were collected between 3 and 12 May 2007 (i.e. at the end of the dry season) from the subsurface waters (0.5 m) at the 14 stations. Water samples for nutrient and chlorophyll analysis, as well as for prokaryotic and viral enumeration, were collected using acid-cleaned sterile bottles. Samples intended for the determination of dissolved inorganic nutrients ($NO_3$-N, $NH_4$-N, $PO_4$-P) underwent preliminary filtration through Whatman GF/F fiberglass filters, stored at $-20\,^{\circ}C$ and analyzed according to Strickland & Parson (1968). Chlorophyll *a* concentrations were determined fluorometrically following the filtration of samples through Whatman GF/F fiberglass filters, storage in liquid nitrogen and methanol extraction (Yentsch & Menzel, 1963). Analyses of nutrients and chlorophyll *a* concentrations were performed on a single sample.

## Counts of microorganisms

For the prokaryotic and viral enumeration, aliquot samples of 1.5 mL were fixed with prefiltered (0.02 μm) buffered formaldehyde (2% final concentration), flash frozen in liquid nitrogen [as recommended by Patel *et al.* (2007)], stored at −20 °C and analyzed within a maximum of 4 weeks after collection. The abundances of planktonic prokaryotes and viruses were determined by standard techniques using SYBR Gold and epifluorescence microscopy (Patel *et al.*, 2007). The number of virus-like particles and prokaryotes contained in triplicate samples of 50–300 μL were determined after particle retention of the particles on 0.02-μm pore-size membranes (Anodisc) and staining with SYBR Gold. On each slide, 300–600 prokaryotes and viruses were counted under an Olympus Provis-AX70 epifluorescence microscope with blue excitation, in 20 fields.

Water samples (100 mL) dedicated to heterotrophic nanoflagellates (HNF) enumeration were fixed with glutaraldehyde (1% final concentration) and stored at 4 °C. Subsamples of 15–20 mL of preserved water were stained with 4′,6-diamidino-2-phenylindole (DAPI) (final concentration, 15 μg mL$^{-1}$) for 15 min, filtered onto black Nuclepore filters (0.8 μm pore size), stored at −20 °C and counted under the epifluorescence microscope with UV excitation (Sherr *et al.*, 1993). On each slide, 50–200 fields were observed according to cell densities.

Subsamples (50 mL) were fixed with a solution of formaldehyde and sodium borate (final concentration, 4%), and phytoplankton species were analyzed and counted using an inverted microscope Olympus IMT-2 (Utermöhl, 1958). Species were identified according to Bourrelly (1990).

## Viral morphology

The morphology of viruses was determined using transmission electron microscopy (TEM) after they were concentrated using the pegylation method (Colombet *et al.*, 2007). Briefly, following successive prefiltration steps (0.2-μm pore-size filter at the end), viruses contained in 30-mL subsamples were reconcentrated by polyethylene glycol (PEG) precipitation immediately after sampling. PEG 8000 (Sigma) was added to the water sample (final concentration, 10%) and incubated at 4 °C in the dark for 2 weeks. The white phase containing crystallized viruses was pipetted, centrifuged at 8000 ***g*** for 25 min at 4 °C and resuspended in 0.02 μm filtered water. KCl (1 M) was then added to this solution, incubated on ice for 20 min and centrifuged (12 000 ***g***) for 10 min at 4 °C. The supernatant comprised of clean viruses was finally used for morphological diversity analysis by TEM. Viruses were collected onto a 400 mesh Cu electron microscopy grid supported with a carbon-coated Formvar film (Pelanne Instruments, Toulouse, France). The viral concentrate was then centrifuged at 120 000 ***g*** for 2 h, 4 °C using an SW 40 Ti rotor (LE 80K, Beckman). Each grid was stained at room temperature for 30 s with uranyl acetate (2% w/w), rinsed twice with 0.02 μm filtered distilled water and dried on a filter paper. Grids were examined using a JEM 1200EX transmission electron microscope (JEOL) operated at 80 kV at a magnification of ×40 000–80 000. The different viral morphotypes were distinguished on the basis of the size and shape of the tail that typically makes it possible to identify phages belonging to the families of *Myoviridae*, *Siphoviridae* and *Podoviridae*. Tailless viruses were classified as icosahedral-, spherical-, filamentous- and lemon-shaped morphotypes.

## Prokaryotic heterotrophic production (PHP)

PHP was estimated using the [$^3$H]-thymidine incorporation method as developed by Fuhrman & Azam (1982) and modified by Bouvy *et al.* (2004) for tropical systems. For each sample, two 3 mL replicates and one formalin-fixed control were incubated with 100 μL of [$^3$H]-thymidine (47 Ci mmol$^{-1}$, Amersham, UK) and kept in the dark at *in situ* temperature. The final total thymidine concentration was 20 nM. Incubations were stopped after 30 min by adding trichloroacetic acid (final concentration of 5%). Samples were precipitated on ice for 15 min and then filtered through cellulose nitrate filters (pore size, 0.2 μm, Whatman). The filters were then rinsed five times with 3 mL volumes of 5% trichloroacetic acid. The filters were placed in scintillation vials and solubilized with 0.5 mL of ethyl acetate. Six milliliters of a scintillation cocktail (Ready Save, Beckman) was added to each vial, and the radioactivity was measured using a liquid scintillation counter.

## Catalyzed reporter deposition (CARD)-FISH analyses of phylogenetic diversity

Five milliliter samples were fixed with formaldehyde (2% final concentration), filtered on 0.2-μm polycarbonate filters (Whatman) and kept at −20 °C until hybridization. Several horseradish peroxidase probes (Biomers) were used, following Pernthaler *et al.* (2004): EUB 338III, ALF968, BET42a, GAM42a and ARCH915, targeting, respectively, the Eubacteria, the *Alpha*-, *Beta*- and *Gammaproteobacteria* (ALPHA, BETA, GAMMA), the *Bacteroidetes* and the Archaea domain. The NON338 probe was used as a negative control. After permeabilization with lysozyme (10 mg mL$^{-1}$, 1 h at 37 °C; Euromedex) and achromopeptidase (60 U mL$^{-1}$, 30 min at 37 °C; Sigma), seven filter sections, corresponding to the seven selected probes, were cut and hybridized for 2 h at 35 °C (Pernthaler *et al.*, 2004). Probes BET42a and GAM42a were used with competitor oligonucleotides as described in Manz *et al.* (1992). Filter portions were then counterstained with DAPI (1 μg mL$^{-1}$; Euromedex) before enumeration with the epifluorescence microscope. A

minimum of 10 fields per filter-portion was counted. The selected groups were counted and expressed as a percentage relative to the DAPI-stained bacterial cells. The error associated with replicate CARD-FISH counts ranged from 5% to 25% (mean = 10.3%) based on a subset of three samples for which we conducted independent replicate CARD-FISH counts. The error on the percentage of bacteria was 15.3%, and corresponded to the sum of the errors for the bacterial group counts and for the total bacterial counts (average 5%), according to standard propagation of error. This error was consequently applied to all CARD-FISH analyses.

### CTC-positive (CTC+) cells

The proportion of respiring bacteria that have high rates of metabolism was determined using 5-cyano-2,3-ditolyl tetrazolium chloride (CTC), an indicator of the respiratory electron transport system activity (Sherr *et al.*, 1999). Active cells reduce the tetrazolium salt CTC to its fluorescent formazan form, and the cells with a high respiration rate or metabolism produce enough intracellular red fluorescence to allow detection and enumeration by flow cytometry (del Giorgio *et al.*, 1997). A stock solution of 50 mmol $L^{-1}$ CTC (tebu-bio SAS) was prepared daily, filtered through 0.1-μm filters and kept in the dark at 4 °C until use. CTC stock solution was then added to 0.45 mL of sample (5 mmol $L^{-1}$ final CTC concentration) and incubated for 3 h at room temperature in the dark. At the end of the incubation, fluorescent 0.94-μm-diameter beads (Polyscience Inc.) were added as an internal standard before analysis on the cytometer. The red fluorescence of CTC (FL3) and the light scatter SSC were used to discriminate the CTC+ cells from other cells or weak fluorescent particles. The percentage of CTC+ cells, based on triplicate analyses, was calculated relative to the total bacterial counts obtained by epifluorescence microscopy.

### Viral infection of prokaryotes

Prokaryotes contained in duplicate 8 mL aliquots of formalin-fixed samples were harvested by ultracentrifuging at 70 000 ***g*** for 20 min onto 400 mesh Cu grids, stained for 30 s with uranyl acetate (2% w/w) and examined at × 40 000 by TEM operated at 80 kV to distinguish between visibly infected and uninfected prokaryotes (Bettarel *et al.*, 2004). At least 600 prokaryote cells were inspected per grid. Burst size (BS, viruses per bacteria) was estimated for every single sample as the average number of viral particles in all visibly infected prokaryotes totally filled with viruses. The fraction of lytically infected cells (FIC) was calculated from the frequency of visibly infected cells (FVIC) (as a percentage) using the formula: FIC = 7.11 × FVIC (Weinbauer *et al.*, 2002).

### Fraction of lysogenic prokaryotes

We used the method of Jiang & Paul (1996) to initiate prophage induction in prokaryotes. Mitomycin-C (1 μg $mL^{-1}$ final concentration, Sigma Chemical Co., No. M-0503) was added to duplicate 10 mL volumes of water. Duplicate untreated samples served as the control. All samples were formalin fixed after being incubated for 12 h in the dark, at *in situ* temperature. Prophage induction was calculated as the difference in viral abundance between the mitomycin-C treated ($V_m$) and control incubations ($V_c$). The fraction of lysogenic prokaryote cells (FLC) was calculated as

$$\mathrm{FLC}(\%) = 100[(V_m - V_c)/(\mathrm{BS} \times \mathrm{PA}_{t0})]$$

where BS is the burst size (virus per bacteria) and $PA_{t0}$ the prokaryote abundance at the start of the experiment, i.e. before adding mitomycin-C (Weinbauer *et al.*, 2003).

### Persistence of free viruses in water

In 100-mL samples, free viruses were isolated from their hosts by successively filtrating the water through 5.0- and 0.2-μm polycarbonate membranes (47 mm in diameter) to remove prokaryotes and larger organisms. Each 0.2 μm filtrate was placed in a 100-mL polyethylene UV-permeable sterile Whirl-Pack® bag and was incubated for 12 h in the dark. The incubation time of 12 h was chosen to limit the potential repopulation from the small fraction of prokaryotes that may have passed through the 0.2-μm membrane filters (this was checked by an epifluorescence microscopic prokaryote count). The survival rates of viruses (SR%) were calculated as follows

$$\mathrm{SR}(\%) = 1 - [(\mathrm{VIR}_{T0h} - \mathrm{VIR}_{T12h})/\mathrm{VIR}_{T0h}] \times 100$$

where VIR is the viral abundance (expressed in $10^7$ particles $mL^{-1}$).

### Statistical analyses

Data were log transformed to satisfy the requirements of normality and homogeneity of variance necessary for parametric analyses. Simple relationships between original data sets were tested using Pearson correlation analysis. All statistical analyses were performed using SIGMASTAT software.

## Results

### Abiotic parameters

Nutrients exhibited different patterns throughout the gradient, reaching their maximum concentration at salinities 30‰, 190‰ and 360‰, for nitrite+nitrate, ammonium and phosphate, respectively (Table 1). Chlorophyll *a* concentrations were also highly variable, peaking at salinities 30‰, 190‰ and 290‰. Temperature ranged from 22.9 to 29.1 °C,

with the highest values recorded in the shallow crystallizer ponds of Kaolack (Table 1).

## Abundance of viruses, prokaryotes and HNF

Viral abundance increased up to 50-fold between both the extremities of the gradient (Fig. 2a). Although the concentrations were relatively stable between 10‰ and 240‰ of salinity, a sharp increase was observed at the top end of the gradient, with concentrations reaching up to $6.8 \times 10^8$ viruses $mL^{-1}$ at 360‰ (Fig. 2a). A similar pattern was observed for prokaryotes, which increased regularly from salinity 240‰ to attain $3.4 \times 10^8$ cells $mL^{-1}$ at 360‰ (Fig. 2b). The virus and prokaryote counts were highly significantly correlated ($r = 0.99$, $P < 0.001$, Table 2). Conversely, the abundance of HNF declined steadily from 564 to 7 cells $mL^{-1}$, as the salinity increased from 10‰ to 360‰ (Fig. 2c). Phytoplankton abundance increased steadily from $1.5 \times 10^5$ to $9.8 \times 10^7$ cells $L^{-1}$ between salinity 10‰ and 140‰ where picophytoplankton species were dominant (data not shown). Algal abundance showed marked variations throughout the end of the gradient, with values reaching $1.9 \times 10^6$ cells $L^{-1}$ in water approaching salt saturation (Fig. 2d). From salinity 240–360‰, the phytoplankton assemblage was mainly comprised of the green algae *Dunaliella salina* (18–99% of the total abundance) and of *Cyanophyceae* (data not shown).

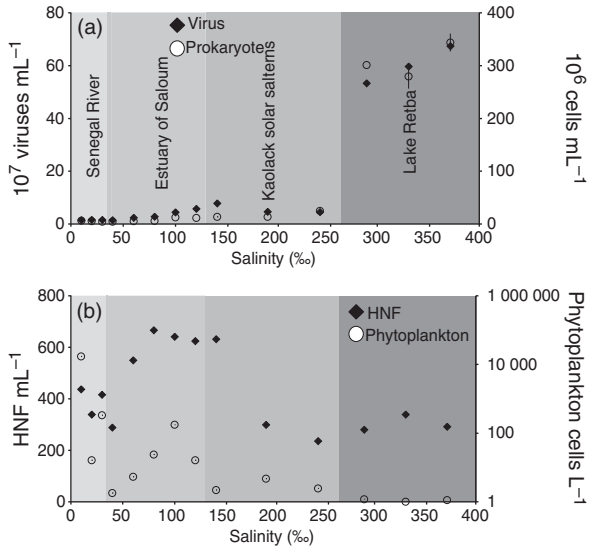


**Fig. 2.** Distribution of viruses, prokaryotes (a), heterotrophic nanoflagellates (HNF) and phytoplankton (b) abundances, along the salinity gradient. Error bars represent the SD of triplicate samples. Note that when no error bar is visible, it is because the error is smaller than the symbol in the graph.

## Prokaryote activity and physiological state

The PHP and the percentage of CTC+ cells followed the same pattern characterized by a general decrease in the values between salinities 10–20‰ and 240‰, followed by a moderate increase from 240‰ to 340‰ (Fig. 3). The proportion of CTC+ cells was between 1.0% and 32.5%; the highest percentage was recorded at salinity 20‰ in the Senegal River, and then CTC+ cells declined steadily down to 1.0% at salinity 120‰. Over the second part of the salinity gradient (120–360‰), CTC+ then increased again to attain 15.9% in Lake Retba. PHP followed the same trend; however, its decrease continued up to salinity 240‰ and then increased again up to 360‰ (Fig. 3).

## Prokaryote community composition and distribution

The proportion of Eubacteria ranged between 15.9% and 92.4% of the total prokaryotic assemblage. Eubacteria sharply declined at salinity 140‰, and then increased throughout the end of the gradient (Fig. 4a). Among the Eubacteria, there was a change in the phylogenetic dominance of the *Alphaproteobacteria*, *Gammaproteobacteria* and *Bacteroidetes* at salinities 30‰, 80‰ and 330‰, respectively (Fig. 4b). Archaea represented from 0.4% to 57% of the total cell counts. Their proportion was marginal up to salinity 110‰, and then increased continuously with increasing salinity up to near-saturation levels (360‰). Square-shaped cells emerged at salinity 190‰, where they accounted for up to 58% of the prokaryotes. From there on, along the gradient, these atypical cells constituted from 28% to 40% of the prokaryotes (Fig. 4c). The distribution of square-shaped cells was closely correlated with that of Archaea ($r = 0.87$, $P < 0.05$) and with salinity levels ($r = 0.79$, $P < 0.05$) (Table 2). Total percentages of Eubacteria and Archaea higher than 100% were due to fluorescent hybridization count errors. On one single occasion (S.190), the proportion of SHOW cells was higher than that of the archaeal cells detected using the ARCH915 probe. However, this probe has been shown to efficiently hybridize square cells inhabiting crystallizer ponds (Antón *et al.*, 1999), dismissing possible specificity problems. This discrepancy is thus more likely caused by the presence of organic aggregates in that station, which may have covered and hidden a significant fraction of the hybridized cells.

## Viral life strategies

Between salinity levels of 10‰ and 140‰, the FIC oscillated from 0.8% to 20.1%, peaking twice at salinities 10‰ and 120‰, respectively (Fig. 5a). Then, in the terminal part of the salinity gradient (i.e. from 190‰ to 360‰), no visibly infected cells were detected among the 9453 prokaryotes that

**Table 2.** Correlation relationships of basic parameters estimated in the surface water of the 14 study stations

| | Salinity | [VIR] | [PROK] | [HNF] | [CHLORO] | SR | $PO_4$ | $NO_2$+$NO_3$ | $NH_4$ | FIC | FLC | PHYTO | [ARCH] | PHP | CTC+ | SHOW | TEMP |
|---|---|---|---|---|---|---|---|---|---|---|---|---|---|---|---|---|---|
| Salinity | **1** | | | | | | | | | | | | | | | | |
| [VIR] | **0.86** | **1** | | | | | | | | | | | | | | | |
| [PROK] | **0.87** | **0.99** | **1** | | | | | | | | | | | | | | |
| [HNF] | −0.65 | −0.48 | −0.50 | **1** | | | | | | | | | | | | | |
| [CHLORO] | 0.30 | 0.43 | 0.36 | −0.19 | **1** | | | | | | | | | | | | |
| SR | **0.92** | **0.89** | **0.89** | −0.51 | 0.40 | **1** | | | | | | | | | | | |
| $PO_4$ | 0.64 | **0.78** | **0.78** | −0.31 | 0.13 | 0.59 | **1** | | | | | | | | | | |
| $NO_2$+$NO_3$ | −0.24 | −0.07 | −0.06 | 0.43 | 0.07 | −0.24 | −0.10 | **1** | | | | | | | | | |
| $NH_4$ | 0.09 | −0.16 | −0.15 | −0.09 | 0.35 | 0.02 | −0.14 | −0.18 | **1** | | | | | | | | |
| FIC | −0.64 | −0.40 | −0.42 | **0.79** | −0.15 | −0.48 | −0.23 | 0.40 | −0.20 | **1** | | | | | | | |
| FLC | 0.34 | 0.11 | 0.08 | −0.26 | **0.69** | 0.31 | −0.10 | −0.21 | **0.82** | −0.34 | **1** | | | | | | |
| PHYTO | 0.46 | 0.42 | 0.41 | −0.34 | 0.58 | 0.36 | 0.41 | −0.37 | 0.47 | −0.32 | 0.53 | **1** | | | | | |
| [ARCH] | **0.96** | **0.88** | **0.89** | −0.58 | 0.43 | **0.95** | 0.66 | −0.14 | 0.24 | −0.58 | 0.45 | 0.49 | **1** | | | | |
| PHP | 0.47 | **0.81** | **0.81** | −0.19 | 0.43 | 0.62 | 0.48 | 0.20 | −0.34 | −0.11 | −0.11 | 0.11 | 0.55 | **1** | | | |
| CTC+ | −0.23 | 0.12 | 0.10 | 0.10 | 0.22 | 0.04 | 0.21 | 0.48 | −0.18 | 0.48 | −0.21 | −0.20 | −0.07 | 0.35 | **1** | | |
| SHOW | **0.78** | 0.60 | 0.59 | −0.49 | 0.60 | **0.77** | 0.45 | −0.24 | 0.60 | −0.52 | **0.80** | 0.58 | **0.87** | 0.23 | −0.13 | **1** | |
| TEMP | **0.71** | 0.33 | 0.35 | −0.55 | 0.19 | 0.47 | 0.15 | −0.24 | 0.43 | −0.62 | 0.59 | 0.51 | 0.66 | −0.11 | −0.51 | **0.69** | **1** |

VIR, viruses; PROK, prokaryotes; SR, viral survival rates; ARCH, Archaea; TEMP, temperature. Significant correlations ($P < 0.01$) are indicated in bold.

were examined. A negative correlation was found between FIC and salinity ($r = -0.68$, $P < 0.05$, Table 2). Although the relationship was not significant, the dynamics of the FLC tended to be the opposite of that of FIC. Indeed, FLC remained relatively low up to salinity 140‰ (0.5–5.9%), and then peaked at salinity 190% to reach 62.9%, before declining steeply throughout the rest of the gradient. FLC was positively correlated with the abundance of the square prokaryotes ($r = 0.75$, $P < 0.05$, Table 2).

### Viral persistence in water

The survival of free viruses after 12 h slowly decreased between the salinities 10‰ and 140‰, with survival rates ranging from 53.4% to 30.2% (Fig. 5b). Viral persistence then increased steadily up to 97.5% at the highest salinities in Lake Retba. Positive and significant correlations were found between viral persistence and (1) salinity, (2) the proportion of square cells and (3) the proportion of Archaea (Table 2).

### Viral morphological diversity

Although tailless icosahedral viruses declined between 10‰ and 240‰ of salinity, they remained highly dominant, accounting for 58–86% of virioplankton standing stocks (Fig. 6). At salinities $> 240$‰, the incidence of these viruses declined sharply and finally disappeared at near salt saturation, in Lake Retba. The same situation was observed for *Myoviridae*, *Siphoviridae* and *Podoviridae*, whose presence was quasi negligible between salinities 240‰ and 360‰. Conversely, spindle-shaped viruses emerged in moderate amounts at salinity 240‰ (mean = 3%), but were dominant along the end of the salinity gradient, in Lake Retba (Fig. 6). In this hypersaline lake, other viral morphotypes typical of archaeal viruses were also detected at high levels of abundance: filamentous and spherical viruses that accounted for up to 20% and 33%, respectively (Figs 6 and 7).

## Discussion

### Ecological traits of prokaryotes along the salinity gradient

As reported frequently in the literature, the abundance of the prokaryotes gained two orders of magnitude from freshwater to hypersaline stations, reaching up to $3.4 \times 10^8$ cell mL$^{-1}$, which is roughly 100-fold higher than what is generally found in marine environments (Suttle, 2005). In this study, while prokaryotic abundance increased steadily up to salinity 240‰, conversely, their physiological state, as reflected by the proportion of CTC+ cells, and the PHP both decreased. We can surmise that the osmotic stress exerted on prokaryotes may directly limit their metabolic

activity. Halophilic prokaryotes can avoid water loss and adjust their turgor pressure in a highly saline environment by accumulating osmotically active compounds such as glycine betaine, glutamate, glutamine and proline (Sleator & Hill, 2001; Burkhardt *et al.*, 2009). When salt stress increases, bacteria may be forced to use energy-consuming mechanisms to maintain the osmotic balance in their cells instead of being able to use this energy for growth. On the basis of our observations, this scenario might be accurate up to salinity 250‰, but beyond this, the tremendous abundance of highly active prokaryotes in the Lake Retba may be attributable to high selection pressure, leading to the development of a unique assemblage of highly adapted, fast-growing and active cells, as reported previously by Guixa-Boixareu *et al.* (1996). It is also possible that most of the bacterial populations that survived at salinity 200‰ were still somewhat reminiscent of those found in coastal marine waters (Pedrós-Alió *et al.*, 2000), but that only the halophilic species remained active. Although salinity 250‰ seems to correspond to the threshold beyond which both prokaryote abundance and metabolism intensify, we observed that marked phylogenetic changes occurred earlier in the gradient, i.e. at salinity 150‰ (Fig. 4a and b). Between salinities of 0‰ and 150‰, the prokaryote assemblage was dominated by Eubacteria (mostly *Alphaproteobacteria* at salinity 30‰, then *Gammaproteobacteria* at 80‰), and Archaea

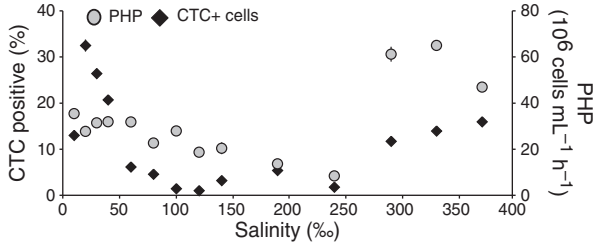


**Fig. 3.** Dynamics of PHP and CTC + cells, along the salinity gradient.

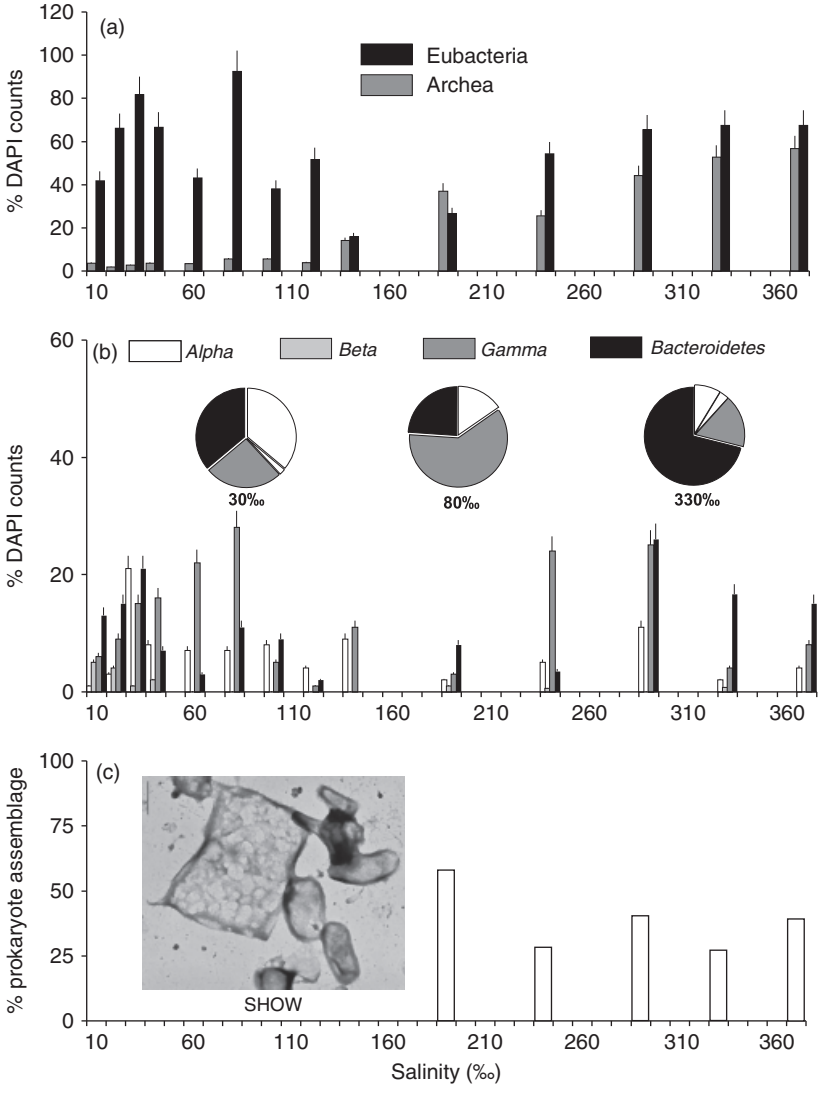


**Fig. 4.** Distribution of the Eubacteria and Archaea along the salinity gradient (a). Phylogenetic distribution among the Eubacteria of the *Bacteroidetes* and the *Alpha*-, *Beta*- and *Gammaproteobacteria* along the salinity gradient (bars). Pies indicate the representative eubacterial community composition at salinities 30‰, 80‰ and 330‰ (b). Micrograph and contribution of the SHOW to the prokaryote assemblage (c). Scale bar = 500 nm.

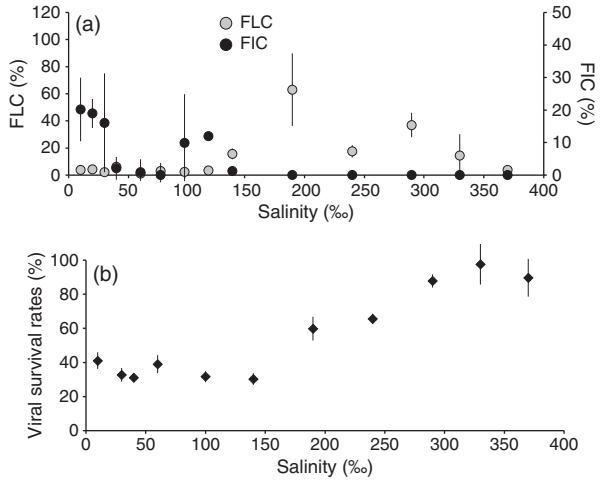


**Fig. 5.** FLC and FIC along the salinity gradient (a). Survival rates (SR%) of free viruses, after 12 h of incubation in the dark (b).

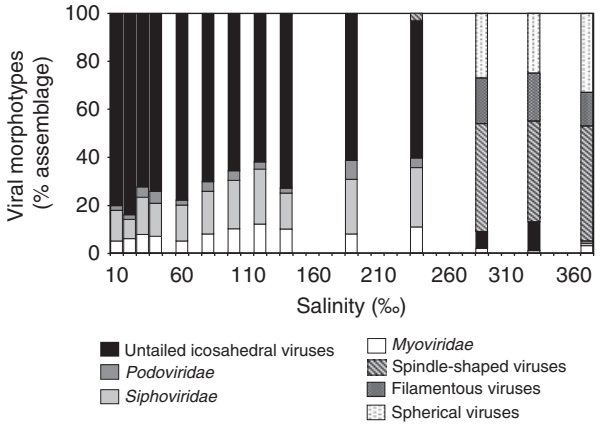


**Fig. 6.** Contribution of the different morphotypes to the viral assemblage along the salinity gradient.

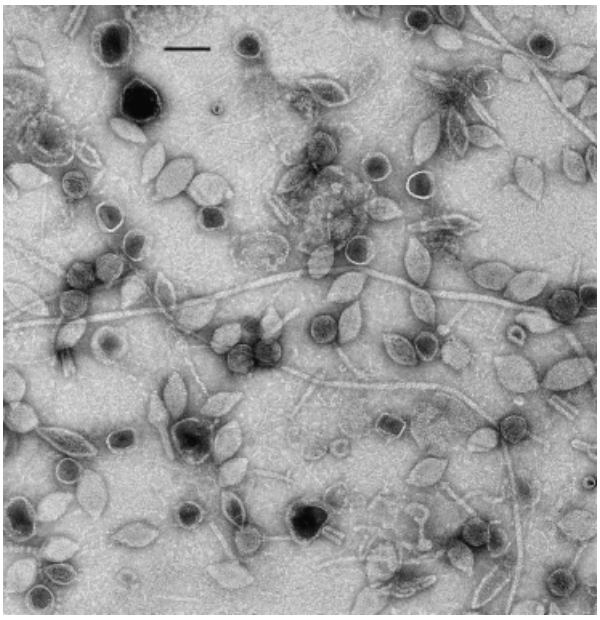

**Fig. 7.** Overview of virus-like particles observed in the Lake Rebta (Senegal) by TEM. Samples contained a mixture of various viruses (including spindle, linear, spherical shaped) that could be distinguished with morphological criteria. Scale bar = 100 nm. See more details in Sime-Ngando *et al*. (2011).

were relatively rare ( $<$ 10% of DAPI counts). Above 150‰ of salinity, the proportion of Archaea increased continuously up to the top of the gradient, where they constituted up to 60% of the prokaryote assemblage, along with the emergence and proliferation of cells with an atypical square shape (Fig. 4c). In two different studies conducted in crystallizer ponds, Antón *et al.* (1999), and then Casamayor *et al.* (2000) also reported that Archaea can account for $>$ 67% of the total DAPI counts where salinity reaches saturation. Cells belonging to the *Bacteroidetes* exhibited a similar pattern characterized by a marked increase at the most salinized sites, constituting up to 28% of the total DAPI counts in the Lake Retba (Fig. 4b). Previous studies have reported that microbial communities in hypersaline environments have a low diversity (Benlloch *et al*., 2002; Maturrano *et al*., 2006), and are typically dominated by a very small number of prokaryote species while maintaining a large biomass: the extreme halophilic rod-shaped bacterium belonging to the *Bacteroidetes* group, *S. ruber* (Antón *et al*., 2002; Rosselló-Mora *et al*., 2008; Sime-Ngando *et al*., 2011), and the square red halophilic archaea, recently isolated and described as SHOW (Walsby, 2005; Burns *et al*., 2007; Cuadros-Orellana *et al*., 2007). In the tropical sites studied, we found strong evidences that the bacterial community were also comprised of these dominant prokaryotes. Indeed, the strong correlation between the abundance of square cells and the proportion of Archaea seemed to indicate the presence of SHOW. From a culture-independent analysis of the microbial diversity in a sample collected in Lake Retba in April 2008, few of the 16S sequences corresponded to known archaeal general (*Haloquadratum*, *Halorubrum* and *Natromonas*), whereas the majority represented novel archaeal clades. The cells in our samples resembled thin, square or rectangular sheets with sharp corners, measuring 1.5–3.0 μm across and contained numerous gas vesicles (see picture in Fig. 4c), which are typical characteristics of the *Halobacteriaceae* (Walsby, 2005).

## Viral dynamics along the salinity gradient

Viral abundance was tightly linked to that of prokaryotes along the salinity gradient with the concentration reaching

up to $6.8 \times 10^8$ particles $mL^{-1}$ at salinity 360‰. Such abundances come as no surprise because hypersaline environments have been well described to harbor huge numbers of viruses, as high as 2 billion particles per milliliter of water (Guixa-Boixareu *et al.*, 1996; Oren *et al.*, 1997; Bettarel *et al.*, 2006; Schapira *et al.*, 2009). Intuitively, such high numbers of halophages might be explained by the high abundance of their prokaryotic hosts, which in turn might be due to the very low abundance of their nanoflagellate predators. This scenario is supported by a previous study where bacterivory could not be detected at salinities $> 200$‰ (Pedrós-Alió *et al.*, 2000). Another potential explanation is that halophages might be more resistant to ambient virucidal agents than their freshwater or marine counterparts. There is some confirmation of this hypothesis in our experiment, where we found that the survival rates of free viruses (i.e. without their hosts) increased significantly from salinity 200‰ and peaked at 340‰. The reasons for such better survival rates in hypersaline habitats remain unclear. We know that viruses are much more resistant to changes in ionic strength conditions than their host cells (Kukkaro & Bamford, 2009), but we can also envisage that viruses inhabiting seemingly inhospitable niches may be genetically distinct, and specifically niche adapted as suggested by Prangishvili *et al.* (2006) and Le Romancer *et al.* (2007). In such high-salinity habitats where potentially virivorous HNF or ciliates cannot live, viruses might also be preserved from predation and this may also contribute to their high abundance. Furthermore, the unicellular *D. salina* was one of the last Eukarya capable of surviving and proliferating at salinities higher than 240‰. *Dunaliella* is known to produce massive amounts of glycerol to ensure osmotic stabilization of the cytoplasm, and this compound is often postulated to be the main source of organic carbon for the heterotrophic prokaryotes in hypersaline ecosystems (Elevi Bardavid *et al.*, 2008). Questionably, glycerol, as demonstrated by Peak & Peak (1980), might also represent a protective substance for viral capsids against virucidal agents such as UV radiation, but also presumably from the ambient proteases or the degradative effects of temperature.

## The 'infectivity' paradox in hypersaline habitats

Certainly, the most intriguing finding in this study is the paradox of high viral concentrations, but low FVIC in high-salinity environments. Indeed, we observed that progressively fewer prokaryotes were visibly infected along the gradient, and infected cells even became undetectable beyond salinity 170‰. From a study conducted in a salt pond in Jamaica, Daniels & Wais (1998) reported that phages of low virulence predominated in culturable populations. The same authors also demonstrated that lytic phages infecting extreme halophilic prokaryotes in hypersaline lagoons do not produce active infections at saturating concentrations of NaCl (Daniels & Wais, 1980). By contrast, a study conducted in solar salterns located in Spain reported that between 1% and 10% of the square cells were filled with lemon-shaped phage particles (Guixa-Boixareu *et al.*, 1996). Therefore, we cannot exclude the possibility that the latent period (during which mature viruses are not yet visible within the host cell) of tropical halophages could be much longer than that is generally reported in the literature for temperate marine or freshwater viruses (Weinbauer *et al.*, 2002). This might partly explain why observations of infected cells in water were so rare in the tropical hypersaline stations, but this has to be further explored.

According to the 'kill-the-winner' hypothesis (Winter *et al.*, 2010), the typically low-diversity prokaryote assemblage in hypersaline habitats (Benlloch *et al.*, 2002) provides a virtually ideal environment for large viral populations (Pedrós-Alió *et al.*, 2000). On the other hand, if the 'kill-the-winner' hypothesis is true, then this dense phage population could rapidly induce dramatic effects in this high-biomass prokaryote community. Guixa-Boixareu *et al.* (1996) have suggested that the occurrence of such abundant pathogens is inconceivable without '*an evasion strategy that promotes variations at the phage attachment sites*'. Daniels & Wais (1998) also suggested that the low virulence of halophages probably arises as a result of slow adsorption processes occurring in hypersaline environment. Interestingly, there have been several reports of high salt concentrations inhibiting the binding of viruses to their hosts (Kukkaro & Bamford, 2009) and this is certainly a promising avenue for further researches to unravel halovirus–haloarchaeon interactions in nature.

The addition of mitomycin-C as a prophage inductor revealed that the percentage of cells at the lysogenic stage of infection was strongly and positively correlated with the proportion of the square cells. Although we know that few of the haloviruses identified have been reported to be strictly lytic (Porter *et al.*, 2007), this study is among the first to report lysogenic-oriented life strategies in haloarchaeophages along salinity gradients. This seems to indicate, as suggested previously by Porter *et al.* (2007), that a substantial fraction of the haloarcheophages may be temperate rather than virulent in habitats where the salinity exceeds 250‰. This is in support of Daniels & Wais (1998) hypothesis that halophages have probably evolved to exert minimal selective pressure on sensitive hosts, by producing active infections mainly when the host is likely to be destroyed by changing environmental conditions. Our samples were collected in late April, at the end of the dry season after 6 months of stable climatic conditions characterized by a total absence of rain and a temperature of between 28 and 34 °C (data not shown). Such stable conditions may thus partly explain why lysogens were detected in Lake Retba before the

occurrence of any natural induction event such as the arrival of the rainy season and the subsequent decline in salinity. Interestingly, phages infecting hyperthermophilic archaea have also been recognized for their lysogenic rather than lytic lifestyle (Prangishvili *et al.*, 2006).

Moreover, during halovirus infection, archaeons that have a distinct thin, glycoprotein surface layer protecting the cell membrane (unlike Bacteria with their rigid peptidoglycan cell walls) have been shown to release viruses continuously without cell lysis, in a manner similar to the situation in chronic infection (Prangishvili *et al.*, 2006; Porter *et al.*, 2007). This strategy could also allow haloarchaea to continue to divide, thus maintaining high abundances of prokaryotes along with their viral pathogens, as hypothesized previously by Daniels & Wais (1980). Therefore, the nearly 1 billion viral particles per milliliter recorded at salinity higher than 300‰ may not result from the release of lytic viruses, but rather from the chronic-like interactions or from sporadic prophage induction, likely coupled with good conditions for viral preservation.

The morphology of planktonic viruses also showed strong salinity-driven dependence with the emergence, $>$ 150‰, of spindle shaped, linear or spherical morphotypes. Although some morphologies found in the Lake Retba were similar to known viruses of hypersaline environment (Dyall-Smith *et al.*, 2003; Santos *et al.*, 2007) or hyperthermophilic archaea (Prangishvili *et al.*, 2006), an unexpected morphological diversity comprising uncommon viruses that did not resemble any known group of virus (hairpin-shaped or bacilliform particles for example) was revealed from Lake Retba that appears to exceed that observed in other saline ecosystems (Sime-Ngando *et al.*, 2011). Currently, about 17 haloarchaeal viruses have been isolated, with the great majority resembling tailed dsDNA bacteriophages, such as λ phages (Porter *et al.*, 2007).

Finally, the constraining pressure that is typically exerted by salt on life forms was successfully faced by prokaryotes and their viral parasites. Both communities displayed remarkable changes in their ecological traits along the salinity gradient and became highly abundant at or near salt saturation. Further studies are now necessary to understand how the coevolution of both communities in hypersaline environments has led to this peculiar type of relationship, seemingly favoring both viral and prokaryotic proliferation.

## Acknowledgements

This study was supported by the GDR CNRS 2476 'Reseaux trophiques Aquatiques' attributed to B. Mostajir, and by Agence National de la Recherche, France, Programme Biodiversité (AQUAPHAGE). We are very grateful to Amy Kirkham for the English revision of the manuscript and to Audrey Rayé, El Hadj N'Dour, Jonathan Colombet, Daniel Corbin and Maïmouna M'Boup for their valuable technical and field assistance.

## References

Antón J, Llobet-Brossa E, Rodríguez-Valera F & Amann R (1999) Fluorescence *in situ* hybridization analysis of the prokaryotic community inhabiting crystallizer ponds. *Environ Microbiol* **1**: 517–523.

Antón J, Oren A, Benlloch S, Rodríguez-Valera F, Amann R & Rosselló-Mora R (2002) *Salinibacter ruber* gen. nov., sp. nov., a novel, extremely halophilic member of the Bacteria from saltern crystallizer ponds. *Int J Syst Evol Micr* **52**: 485–491.

Auguet JC, Montanié H & Lebaron P (2006) Structure of virioplankton in the Charente Estuary (France): transmission electron microscopy versus pulsed field gel electrophoresis. *Microb Ecol* **51**: 197–208.

Benlloch S, Lopez-Lopez A, Casamayor EO *et al.* (2002) Prokaryotic genetic diversity throughout the salinity gradient of a coastal solar saltern. *Environ Microbiol* **4**: 349–360.

Bettarel Y, Sime-Ngando T, Amblard C & Dolan J (2004) Viral activity in two contrasting lake ecosystems. *Appl Environ Microb* **70**: 2941–2951.

Bettarel Y, Sime-Ngando T, Bouvy M, Arfi R & Amblard C (2005) Low consumption of virus-sized particles by heterotrophic nanoflagellates in two lakes of the French Massif Central. *Aquat Microb Ecol* **39**: 205–209.

Bettarel Y, Bouvy M, Dumont C & Sime-Ngando T (2006) Virus–bacterium interactions in water and sediment of West African inland aquatic systems. *Appl Environ Microb* **72**: 5274–5282.

Bettarel Y, Bouvier T & Bouvy M (2009) Viral persistence in water as evaluated from a tropical/temperate cross-incubation. *J Plankton Res* **31**: 909–916.

Bettarel Y, Desnues A & Rochelle-Newall E (2010) Lytic failure in cross-inoculation assays between phages and prokaryotes from three aquatic sites of contrasting salinity. *FEMS Microbiol Lett* **311**: 113–118.

Boetius A & Joye S (2009) Thriving in salt. *Science* **324**: 1523–1525.

Bolhuis H, Palm P, Wende A *et al.* (2006) The genome of the square archaeon *Haloquadratum walsbyi*: life at the limits of water activity. *BMC Genomics* **7**: 169.

Bourrelly P (1990) *Les Algues d'Eau Douce, Tome I. Les Algues Vertes*, 2nd edn. Boubée et Cie, Paris, France.

Bouvier TC & del Giorgio PA (2002) Compositional changes in free-living bacterial communities along a salinity gradient in two temperate estuaries. *Limnol Oceanogr* **47**: 453–470.

Bouvy M, Troussellier M, Got P & Arfi R (2004) Bacterioplankton responses to bottom-up and top-down controls in a West African reservoir (Selingue, Mali). *Aquat Microb Ecol* **34**: 301–307.

Brum JR, Steward GF, Jiang SC & Jellison R (2005) Spatial and temporal variability of prokaryotes, viruses, and viral

infections of prokaryotes in an alkaline, hypersaline lake. *Aquat Microb Ecol* **41**: 247–260.

Burkhardt J, Sewald X, Bauer B, Saum SH & Müller V (2009) Synthesis of glycine betaine from choline in the moderate halophile *Halobacillus halophilus*: co-regulation of two divergent, polycistronic operons. *Environ Microbiol Rep* **1**: 38–43.

Burns DG, Janssen PH, Itoh T *et al.* (2007) *Haloquadratum walsbyi* gen. nov., sp. nov., the square haloarchaeon of Walsby, isolated from saltern crystallizers in Australia and Spain. *Int J Syst Evol Micr* **57**: 387–392.

Casamayor EO, Calderón-Paz JI & Pedrós-Alió C (2000) 5S rRNA fingerprints of marine bacteria, halophilic archaea and natural prokaryotic assemblages along a salinity gradient. *FEMS Microbiol Ecol* **34**: 113–119.

Cissoko M, Desnues A, Bouvy M, Sime-Ngando T, Verling E & Bettarel Y (2008) Effects of freshwater and seawater mixing on virio- and bacterioplankton in a tropical estuary. *Freshwater Biol* **53**: 1154–1162.

Colombet J, Robin A, Lavie L, Bettarel Y, Cauchie HM & Sime-Ngando T (2007) Virioplankton 'pegylation': use of PEG (polyethylene glycol) to concentrate and purify viruses in pelagic ecosystems. *J Microbiol Meth* **71**: 212–219.

Cuadros-Orellana S, Martin-Cuadrado AB, Legault B, D'Auria G, Zhaxybayeva O, Papke RT & Rodríguez-Valera F (2007) Genomic plasticity in prokaryotes: the case of the square haloarchaeon. *ISME J* **1**: 235–245.

Daniels LL & Wais AC (1980) Ecophysiology of bacteriophage S5100 infecting *Halobacterium cutirubrum*. *Appl Environ Microb* **56**: 3605–3608.

Daniels LL & Wais AC (1998) Virulence in phage populations infecting *Halobacterium cutirubrum*. *FEMS Microbiol Ecol* **25**: 129–134.

del Giorgio PA, Prairie YT & Bird DF (1997) Coupling between rates of bacterial production and the abundance of metabolically active bacteria in lakes, enumerated using CTC reduction and flow cytometry. *Microb Ecol* **34**: 144–154.

Diop ES, Soumare A, Diallo N & Guisse A (1997) Recent changes of the mangroves of the Saloum River Estuary, Senegal. *Mangr Salt Marsh* **1**: 163–172.

Dyall-Smith M, Tang SL & Bath C (2003) Haloarchaeal viruses: how diverse are they? *Res Microbiol* **154**: 309–313.

Elevi Bardavid R, Khristo P & Oren A (2008) Interrelationships between *Dunaliella* and halophilic prokaryotes in saltern crystallizer ponds. *Extremophiles* **12**: 5–14.

Forsyth MP, Shindler DB, Gochnaue MB & Kushner DJ (1971) Salt tolerance of intertidal marine bacteria. *Can J Microbiol* **17**: 825–828.

Fuhrman JA & Azam F (1982) Thymidine incorporation as a measure of heterotrophic bacterioplankton production in marine surface waters – evaluation and field results. *Mar Biol* **66**: 109–120.

Garnier JM (1978) Evolution géochimique d'un milieu confiné: le lac Retba, Senegal. *Rev Geogr Phys Geol* **2**: 43–58.

Guixa-Boixareu N, Calderón-Paz JI, Heldal M, Bratbak G & Pedrós-Alió C (1996) Viral lysis and bacterivory as prokaryotic loss factors along a salinity gradient. *Aquat Microb Ecol* **11**: 215–227.

Jiang SC & Paul JH (1996) Occurrence of lysogenic bacteria in marine microbial communities as determined by prophage induction. *Mar Ecol-Prog Ser* **142**: 27–38.

Kukkaro P & Bamford DH (2009) Virus–host interactions in environments with a wide range of ionic strengths. *Environ Microbiol Rep* **1**: 71–77.

Le Romancer M, Gaillard M, Geslin C & Prieur D (2007) Viruses in extreme environments. *Rev Environ Sci Biotechnol* **6**: 17–31.

Lozupone CA & Knight R (2007) Global patterns in bacterial diversity. *P Natl Acad Sci USA* **104**: 11436–11440.

Manz W, Amann R, Ludwig W, Wagner M & Schleifer KH (1992) Phylogenetic oligodeoxynucleotide probes for the major subclasses of proteobacteria – problems and solutions. *Syst Appl Microbiol* **15**: 593–600.

Maturrano L, Santos F, Rosselló-Mora R & Antón J (2006) Microbial diversity in Maras salterns, a hypersaline environment in the Peruvian Andes. *Appl Environ Microb* **72**: 3887–3895.

Maurice CF, Bouvier T, Comte J, Guillemette F & del Giorgio PA (2010) Seasonal variations of phage life strategies and bacterial physiological states in three northern temperate lakes. *Environ Microbiol* **12**: 628–641.

Oren A (2002) Diversity of halophilic microorganisms: environments, phylogeny, physiology, and applications. *J Ind Microbiol Biot* **28**: 56–63.

Oren A (2009) Saltern evaporation ponds as model systems for the study of primary production processes under hypersaline conditions. *Aquat Microb Ecol* **56**: 193–204.

Oren A, Bratbak G & Heldal M (1997) Occurrence of virus-like particles in the Dead Sea. *Extremophiles* **1**: 143–149.

Patel A, Noble RT, Steele JA, Schwalbach MS, Hewson I & Fuhrman JA (2007) Virus and prokaryote enumeration from planktonic aquatic environments by epifluorescence microscopy with SYBR Green I. *Nat Protoc* **2**: 269–276.

Peak MJ & Peak JG (1980) Protection by glycerol against the biological actions of near-ultraviolet light. *Radiat Res* **83**: 553–558.

Pedrós-Alió C, Calderón-Paz JI, MacLean MH, Medina G, Marrasé C, Gasol JM & Guixa-Boixereu N (2000) The microbial food web along salinity gradients. *FEMS Microbiol Ecol* **32**: 143–155.

Pernthaler A, Pernthaler J & Amann R (2004) Sensitive multi-color fluorescence *in situ* hybridization for the identification of environmental microorganisms. *Molecular Microbial Ecology Manual*, *Vol. 3*, 2nd edn, pp. 711–726. Kluwer Academic Publishers, Dordrecht, The Netherlands.

Porter K, Russ BE & Dyall-Smith ML (2007) Virus–host interactions in salt lakes. *Curr Opin Microbiol* **10**: 418–424.

Prangishvili D, Forterre P & Garrett RA (2006) Viruses of the Archaea: a unifying view. *Nat Rev Microbiol* **4**: 837–848.

Rohwer F & Thurber RV (2009) Viruses manipulate the marine environment. *Nature* **459**: 207–212.

Rosselló-Mora R, Lucio M, Peña A *et al.* (2008) Metabolic evidence for biogeographic isolation of the extremophilic bacterium *Salinibacter ruber*. *ISME J* **2**: 242–253.

Sandaa RA, Skjoldal EF & Bratbak G (2003) Virioplankton community structure along a salinity gradient in a solar saltern. *Extremophiles* **7**: 347–351.

Santos F, Meyerdierks A, Pena A, Rosselló-Mora R, Amann R & Antón J (2007) Metagenomic approach to the study of halophages: the environmental halophage 1. *Environ Microbiol* **9**: 1711–1723.

Schapira M, Buscot MJ, Leterme SC, Pollet T, Chapperon C & Seuront L (2009) Distribution of heterotrophic bacteria and virus-like particles along a salinity gradient in a hypersaline coastal lagoon. *Aquat Microb Ecol* **54**: 171–183.

Shabala L, Bowman J, Brown J, Ross T, McMeekin T & Shabala S (2009) Ion transport and osmotic adjustment in *Escherichia coli* in response to ionic and non-ionic osmotica. *Environ Microbiol* **11**: 137–148.

Sherr BF, del Giorgio P & Sherr EB (1999) Estimating abundance and single-cell characteristics of respiring bacteria via the redox dye CTC. *Aquat Microb Ecol* **18**: 117–131.

Sherr EB, Caron DA & Sherr BF (1993) Staining of heterotrophic protists for visualization via epifluorescence microscopy. *Handbook of Methods in Aquatic Microbial Ecology* (Kemp P, Cole J, Sherr BF & Sherr EB, eds), pp. 213–227. Lewis Publishers, Boca Raton, FL.

Sime-Ngando T, Lucas S, Colombet J *et al.* (2011) Diversity of virus–host systems in hypersaline Lake Retba, Senegal. *Environ Microbiol* DOI: 10.1111/j.1462-2920.2010.02323.x.

Sleator RD & Hill C (2001) Bacterial osmoadaptation: the role of osmolytes in bacterial stress and virulence. *FEMS Microbiol Rev* **26**: 49–71.

Sorokin DY & Kuenen JG (2005) Haloalkaliphilic sulfur-oxidizing bacteria in soda lakes. *FEMS Microbiol Rev* **29**: 685–702.

Strickland JDH & Parson TR (1968) *A Practical Handbook of Seawater Analysis*. Fisheries Research Board of Canada bulletin, Ottawa.

Suttle CA (2005) Viruses in the sea. *Nature* **437**: 356–361.

Talling JF & Lemoalle J (1998) *Ecological Dynamics of Tropical Inland Waters*. University Press, Cambridge.

Utermöhl H (1958) Zur Vervollkommnung der quantitativen Phytoplankton-Methodik. *Mitt Int Ver Theor Angew Limnol* **9**: 1–39.

Walsby AE (2005) Archaea with square cells. *Trends Microbiol* **13**: 193–195.

Weinbauer MG (2004) Ecology of prokaryotic viruses. *FEMS Microbiol Rev* **28**: 127–181.

Weinbauer MG, Winter C & Höfle MG (2002) Reconsidering transmission electron microscopy based estimates of viral infection of bacterioplankton using conversion factors derived from natural communities. *Aquat Microb Ecol* **27**: 103–110.

Weinbauer MG, Brettar I & Höfle MG (2003) Lysogeny and virus-induced mortality of bacterioplankton in surface, deep, and anoxic marine waters. *Limnol Oceanogr* **48**: 1457–1465.

Wilhelm SW, Jeffrey WH, Dean AL, Meador J, Pakulski JD & Mitchell DL (2003) UV radiation induced DNA damage in marine viruses along a latitudinal gradient in the southeastern Pacific Ocean. *Aquat Microb Ecol* **31**: 1–8.

Winter C, Bouvier T, Weinbauer MG & Thingstad TF (2010) Trade-offs between competition and defense specialists among unicellular planktonic organisms: the 'Killing the Winner' hypothesis revisited. *Microbiol Mol Biol R* **74**: 42–57.

Yentsch CS & Menzel DW (1963) A method for the determination of phytoplankton chlorophyll and pheophytin by fluorescence. *Deep-Sea Res* **10**: 221–231.